Characteristics of Brittle Fracture Under Bi-axial Tensile Load†

Yukio UEDA,* Kazuo IKEDA,** Tetsuya YAO,*** Mitsuru AOKI,** Takashi YOSHIE **** and Takao SHIRAKURA**

Abstract

In this paper, brittle fracture initiation characteristics of plate subjected to bi-axial tension is investigated on cruciform specimens of PMMA (polymenthylmethacrylate) and SM41 (mild steel), each of which contains an inclined crack. The brittle fracture tests are conducted on the cruciform specimens at the load ratio of 1/1, 1/2 and 0/1, and also on straight side specimens under uni-axial tension.

The direction of initial crack propagation and the fracture stress are theoretically estimated by applying the following criteria: (1) the maximum tangential stress, $\sigma_{\theta,max}$, (2) the minimum strain energy density factor, S_{min}, and (3) the maximum decreasing rate of total potential energy, $G_{\theta,max}$.

In the case of PMMA, the test results can be explained well in terms of $\sigma_{\theta,max}$, in which a cirtain ambiguity remains. They can be also explained well in terms of S_{min}, except the direction of initial crack propagation in the case of load ratio, 1/2. However, the physical meaning of S_{min} is not understandable. The test results can be explained most clearly by applying $G_{\theta max}$ criterion, in which the value of G_θ is calculated by the finite element method.

In the case of SM41, the direction of initial crack propagation shows a similar tendency as in the case of PMMA. However, the fracture stresses are higher than the predicted ones applying the linear fracture mechanics, when the mode II deformation is predominant. It may be concluded that the critical value of G_θ depends on the value of K_{II}, that is, the critical value increases as the value of K_{II} increases.

1. Introduction

Generally, the fatigue crack initiates in the stress concentrated regions or at defects of various kinds, and propagates in the direction normal to the local maximum principal stress. Meanwhile, the field stress plays an important role in the initiation of brittle fracture from the existing fatigue crack.

Therefore, the direction of initiation of fatigue crack and that of propagation do not always coincide with that of initiation of brittle fracture. When the structures are subjected to external loads in various directions, the component of load in the direction normal to the plane of the notch or crack-like defects is considered to significantly influence brittle fracture strength of the structural members. Then, investigation into brittle fracture behavior has been performed mainly under uni-axial loading normal to the crack, where the opening mode condition is governed. In order to evaluate the brittle fracture strength in more general cases, it has been required to take into account of the influence of shear mode parallel with the plane of the crack, that is sliding and tearing modes.

In fact, the bi-axial load ratio changes depending on the kinds of structures: the ratio is fixed to 1/2 and 1/1 in the cases of cylindrical and spherical pressure vessels, respectively, and it is fluctuating and complicated in the case of ship and other structures.

In this paper, simplifying the loading condition into bi-axial tensions, the brittle fracture initiation characteristics of plate with an inclined notch is investigated. A special attension is payed on the direction of initial crack propagation and the load at fracture under proportional loading of bi-axial tension whose ratios are 1/1, 1/2 and 0/1. Firstly, fracture tests of specimens of PMMA or a perfectly brittle material are conducted and several existing fracture criteria are discussed from the test results. Then, tests of mild steel fractured in a semi-brittle manner, are also conducted, and the test results are compared with those of PMMA.

---

† Received on Sep. 16, 1976

* Proffessor
** Structural Engineering Laboratory, Kobe Steel, Ltd.
*** Research Associate
**** Graduate Student

2. Existing criteria

As for the criteria of brittle fracture under mixed mode stress sytem, there are the folliwing three main ones defined by: (1) the maximum tangential stress, $\sigma_{\theta max}$, proposed by Erdogan and Sih[1], and the modified one by Williams and Ewing[2], (2) the minimum strain energy density factor, S_{min}, propsed by Sih[3] and (3) the maximum decreasing rate of total potential energy, $G_{\theta max}$, by Anderson and et al.[4]. In this chapter, these criteria will be reviewed briefly.

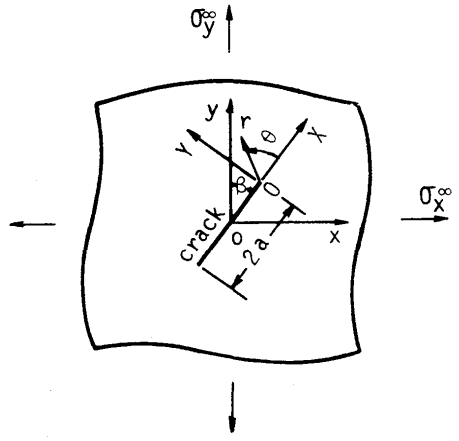

Fig.1 Stress system

2.1 Maximum tangential stress criterion

The tangential stress, σ_θ, in the neighborhood of the crack tip in Fig. 1 can be expressed by

$$\sigma_\theta = \frac{a}{2\sqrt{2r}} \cos\frac{\theta}{2} \left[\sigma_Y(1+\cos\theta - 3\tau_{XY}\sin\theta\right] + \sigma_X \sin^2\theta + \sqrt{\frac{2r}{a}} F(\sigma_Y, \tau_{XY}, \theta) + \cdots\cdots\cdots \quad (1)$$

where

$$\sigma_Y = \sigma_y^\infty \sin^2\beta + \sigma_x^\infty \cos^2\beta$$
$$\sigma_X = \sigma_y^\infty \cos^2\beta + \sigma_x^\infty \sin^2\beta \quad (2)$$
$$\tau_{XY} = (\sigma_y^\infty - \sigma_x^\infty)\sin\beta\cos\beta$$

In the above expression,

r and θ: polar coordinates with the origin 0

σ_x^∞ and σ_y^∞: applied uniform stresses at infinity in the x and y directions, respectively

a: crack half length

σ_X, σ_Y and τ_{XY}: resolved stress components of σ_x^∞ and σ_y^∞ with respect to the X-Y coordinates

β: inclined crack angle to the y-axis.

Using the first term in Eq. (1), Erdogan and Sih proposed the $\sigma_{\theta max}$ criterion. It is restated that a crack will initiate when the maximum value of σ_θ reaches some critical value as a material constant, that is,

$$\sigma_{\theta_0}\sqrt{2r} = \text{const.} \quad (3)$$

This direction, $\theta = \theta_0$, is determined from $\partial\sigma_\theta/\partial\theta = 0$, that is,

$$\sigma_Y \sin\theta_0 - \tau_{XY}(1 - 3\cos\theta_0) = 0 \quad (4)$$

Williams and Ewing also proposed the same criterion using the first two terms in Eq. (1). In this case, the direction of initial crack propagation is obtained from the following equation:

$$\sigma_Y \sin\theta_0 - \tau_{XY}(1-3\cos\theta_0) - \frac{16}{3}\alpha\sigma_X \sin\frac{\theta_0}{2}\cos\theta_0 = 0 \quad (5)$$

where

$$\alpha = \sqrt{2r/a} \quad (6)$$

When Eq. (5) is solved, the value of r should be given. Williams and Ewing maintain that their theoretical prediction is in good agreement with the test results when r is assumed to be 0.05mm. However, the physical meaning of this value is not clarified. In the case of α=0, thier criterion agrees with the one proposed by Erdogan and Sih.

2.2 Minimum strain energy density factor criterion

The amount of strain energy, dW, stored in an infinitesimal element, dA, in the neighborhood of the crack tip as shown in Fig. 2 is given by

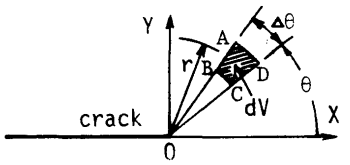

Fig.2 Crack tip element

$$dW = \frac{1}{2}(\sigma_r\epsilon_r + \sigma_\theta\epsilon_\theta + \tau_{r\theta}\gamma_{r\theta})\,dA = \frac{1}{\pi r}(a_{11}K_I^2 + 2A_{12}K_IK_{II} + a_{22}K_{II}^2)\,dA \quad (7)$$

where

σ_r and σ_θ: normal stress components in the polar coordinates

ϵ_r and ϵ_θ: normal strain components in the polar coordinates

$\tau_{r\theta}$ and $\gamma_{r\theta}$: shear stress and strain components in the polar coordinates, respectively

Ki (i=I, II): stress intensity factor for mode i

aij (i, j=1, 2): function of θ and material constants.

The strain energy density factor, S, is defined as

$$S = \frac{1}{\pi}(a_{11}K_I^2 + 2a_{12}K_IK_{II} + a_{22}K_{II}^2) \quad (8)$$

The minimum strain energy density factor, S_{min}, criterion is restated that a crack will initiate in the direction of minimum S.E.D.F. when S_{min} reaches a critical values, S_{cr}, which is a material constant,

$$S_{min} = S_{er} \tag{9}$$

However, the physical background of this criterion should be discussed in future.

2.3 Maximum decreasing rate of total potential energy criterion

The maximum decreasing rate of total potential energy, $G_{\theta max}$, criterion is restated as follows: a crack will initiate in the direction of the maximum value of G_θ, which is the decreasing rate of the total potential energy, when $G_{\theta max}$, reaches a critical value, G_{cr}, which is a material constant, that is,

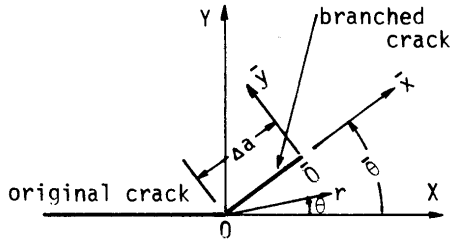

Fig.3 Geometry and coordinate system for the branched crack

$$G_{\theta max} = G_{cr} \tag{10}$$

G_θ is evaluated as the work done to close the infinitesimal branched crack, in Fig. 3, by unit length, which is equivalent to one half of the product of the stresses in the neighborhood of the original crack tip and the opening displacements of the branched crack.

However, it is difficult to obtain the analytical solution of G_θ, bacause that of the crack opening displacements of the branched crack is not available.

On the other hand, Anderson et al.[5] have solved this problem by using the total energy method proposed by Dixon and Pook[6]. In this method, when crack propagates by an infinitesimal length, Δa, in an arbitrary direction, θ, from the original crack tip under a constant load, one half of the external work during the propagation of the crack is equal to the amount of G_θ,

$$G_\theta = \frac{1}{2} \sum_{i=1}^{n} \frac{P_i \Delta \delta_i}{\Delta a} \tag{11}$$

where

P_i: external load vector acting at the point i

$\Delta \delta_i$: change in displacement of the point i as the crack propagates by an infinitesimal length, Δa

n: number of points where the external loads are applied.

3. Test

3.1 Materials

The chemical compositions and mechanical properties of PMMA and mild steel, SM41 are shown in Fig. 4. A series of the deep notch test is conducted to determine the test temperature for the bi-axial test and to obtain the fracture toughness of SM41.

3.2 Test specimens

Two kinds of test specimens are shown in Fig. 5. One is cruciform and the other is straight side. Each one contains a center notch inclined at an angle, β, to the vertical direction, which is machined through thickness. The cruciform one is tested under bi-axial loading, while the

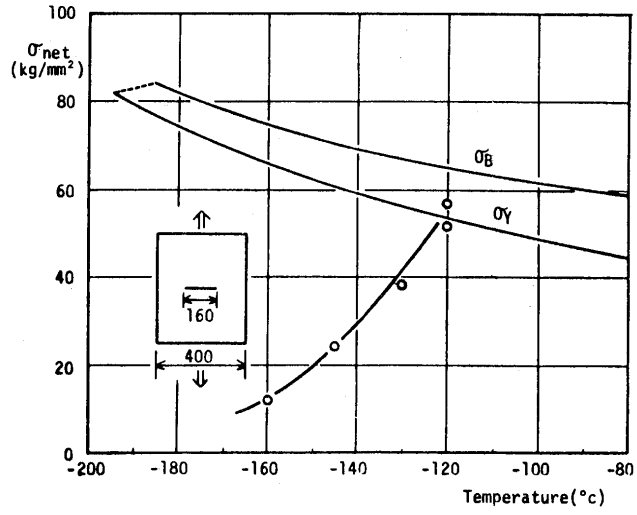

Fig.4 Results of deep notch test

Table 1 Mechanical properties & Chenical compositions

Material	Mechanical Properties			Chemical Composition (%)				
	σ_Y (kg/mm²)	σ_B (kg/mm²)	EL. (%)	C	Si	Mn	P	S
PMMA	——	5.11	1.35	————				
SM41	41	50	26	0.14	0.25	0.86	0.028	0.014

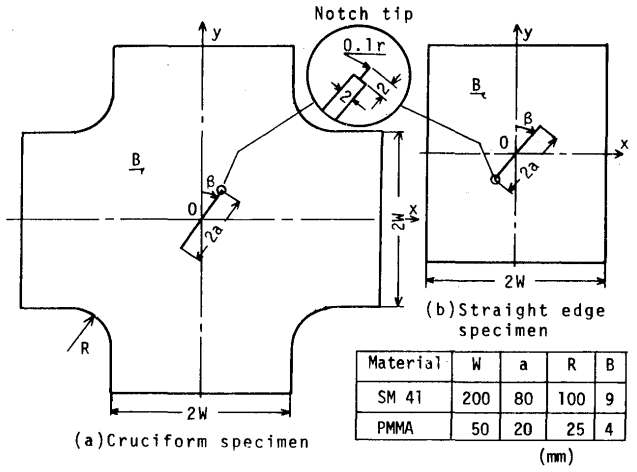

Material	W	a	R	B
SM 41	200	80	100	9
PMMA	50	20	25	4

Fig.5 Detail of test specimen

straight side one is for uni-axial loading. The fracture tests are conducted in the various combinations of the crack angle, β, and the bi-axial load ratio.

3.3 Test procedures

The fracture tests of PMMA were conducted at room temperature. For this tests, a 10 ton vertical testing machine which is controled by displacement is employed for one direction, and for the other one, a load is applied by specially designed screw-type loading apparatus.

The tests of SM41 were performed at approximately constant temperature of $-140°C$ which results in brittle fracture of the specimens with a small scale yielding, as shown in Fig. 4. A 300 ton vertical testing machine is used, with a combination of a specially designed 150 ton horizontal testing machine which can move during testing in accordance with the vertical displacement of the specimen. The appearance of a set of the bi-axial testing machines with capacities of 300 tons and 150 tons, which are installed at Welding Research Institute of Osaka University is shown in Fig. 6.

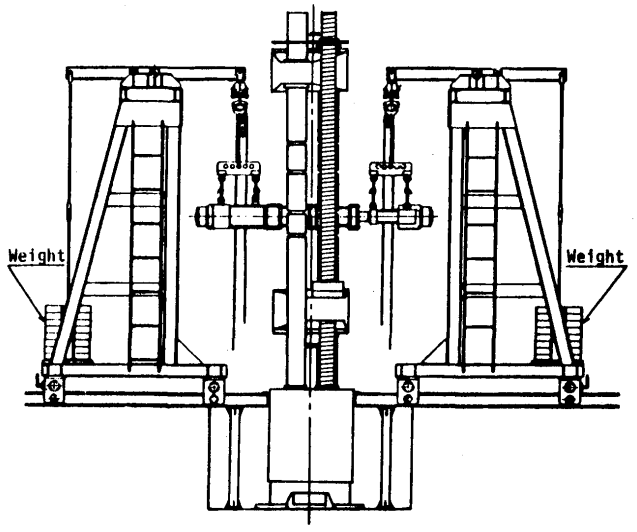

Fig.6 Appearance of testing machine for bi-axial tension

By these tests, the direction of propagation of the initial crack and the fracture load are investigated.

In order to examine the stress distribution in the cruciform specimens, strains in the specimen are measured by means of SR4-strain gages mounted on both surfaces of the specimen, under applying tensions, Px and Py, in the two directions, x and y. The load ratios, Px/Py, are 0/1, 1/2 and 1/1. One of the results at the load ratio, Px/Py of 1/1 is shown in Fig. 7. The stress distribution in the central portion of the specimen can be found to be almost uniform for any load ratios. This stress level in the direction of y-axis reduces approximately to 80%, 76% and 71% of the applied mean stress at the loading edge in the case of Px/Py is equal to 0/1, 1/2 and 1/1, respectively.

4. Test results and discussion

4.1 Stresses surrounding the notch

As mentioned in the preceding chapter, the stresses in the central portion of the cruciform specimens are lower than those averaged at the loading edges. Therefore, it is necessary to know the equivalent stresses on the specimens at fracture to those in the case of an infinite plate, in order to compare the observed fracture stress and the direction of initial crack propagation with those predicted by the three criteria mentioned in Chapter 2. According to the results of a stress analysis by using the finite element method, the average stresses in the central

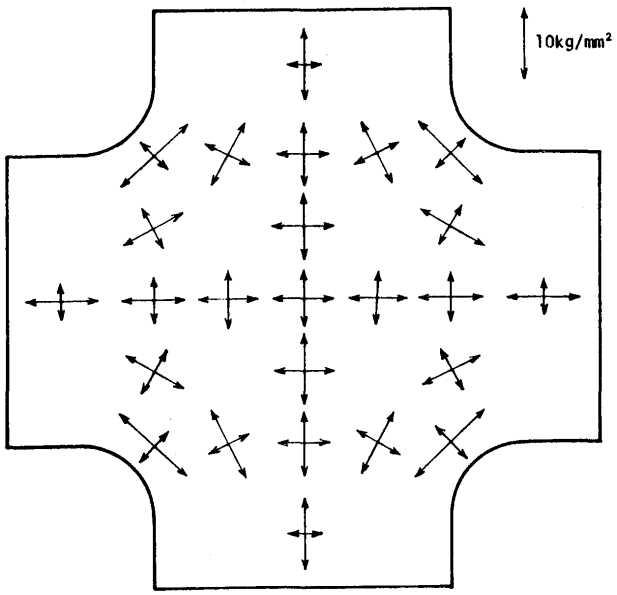

Fig.6 Distribution of principal stresses

portion of the cruciform specimens, σ_{ex} and σ_{ey}, are expressed with the mean stresses at the loading edges, σ_x and σ_y, in the matrix form as follows:

$$\begin{Bmatrix}\sigma_{ex}\\ \sigma_{ey}\end{Bmatrix}=\begin{bmatrix}0.80 & -0.09\\ -0.09 & 0.80\end{bmatrix}\begin{Bmatrix}\sigma_x\\ \sigma_y\end{Bmatrix} \tag{12}$$

These values are only effective to the particular specimens used here, and nearly coincide with the measured ones shown in Section 3.3. It is noted from this result that the stress ratios, σ_{ex}/σ_{ey}, are −0.11 and 0.41 when the load ratio, Px/Py, are 0/1 and 1/2, respectively.

On the other hand, it is necessary to consider the effect of finite width of specimens in the case of straight side specimens. In this case, the ratio of the crack length to the plate width is equal to or less than 0.4, and the correction factor of the finite width for the stress intensity factor is at maximum 1.07, by employing the Irwin's tangential formula. When the cruciform specimens are considered, this finite width is larger than the case of straight side ones, and consequently the correction factor is less than 1.07. These correction factors are small, and their effects are ignored in the following discussion.

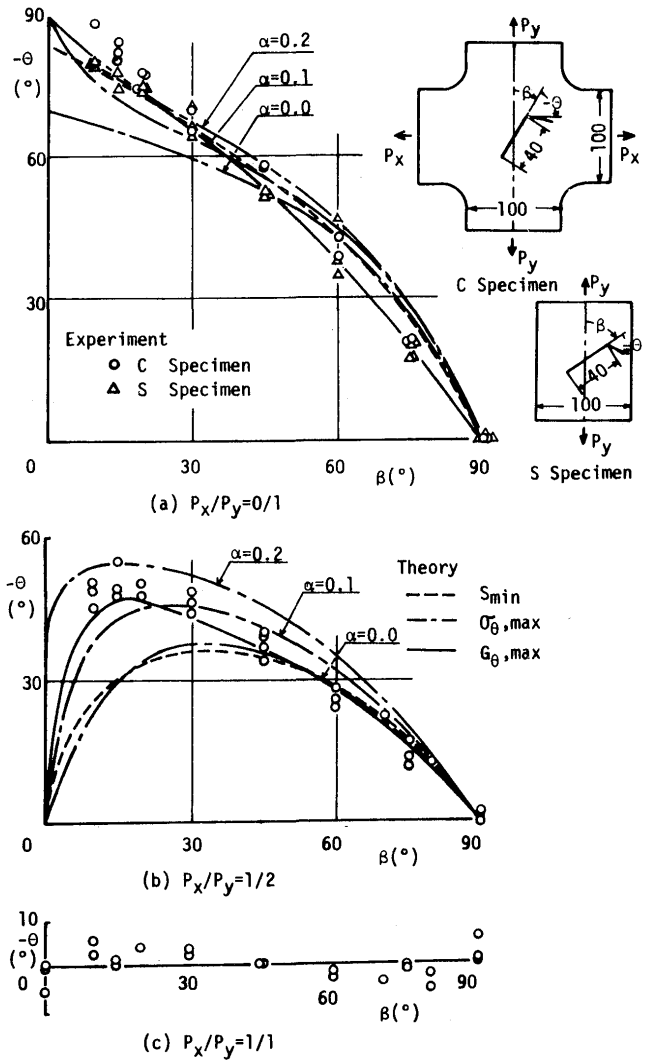

Fig.8 Direction of crack propagation (PMMA)

4.2 Characteristics of brittle fracture on PMMA specimens under mixed mode stress system

The test results from 83 PMMA specimens including the cruciform and straight side ones are summarized in Fig. 8 and 9. In Figs. 8 (a), (b) and (c), the direction of initial crack propagation is plotted against the crack angle,

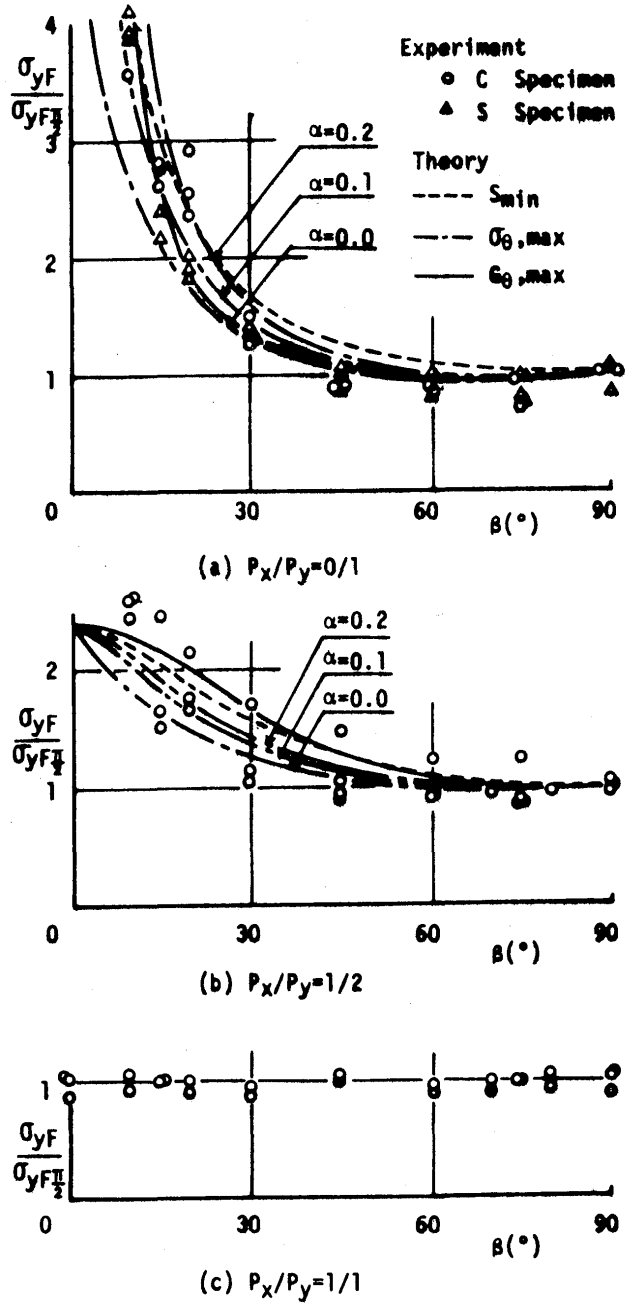

Fig.9 Fracture stresses non-dimensionalyzed by fracture stresses of specimen of ß=90°(PMMA)

β, for the load ratios of 0/1, 1/2 and 1/1, respectively. The curves in these figures are those precdicted by the three criteria mentioned in Chapter 2, and are discussed later in comparison with the test results. When the load ratio is 1/1, the fracture angle curves obtained from $\sigma_{\theta\,max}$ criterion and S_{min} criterion coincide with each other, and are represented with one curve. ($-\theta_0=0°$) In the case of uni-axial tension, the direction of initial crack propagation is almost normal to the loading direction regardless of crack angle, β. ($\beta-\theta_0\fallingdotseq 90°$) When the load ratio is 1/1, the direction of initial crack propagation almost coincides with the original crack line. ($-\theta_0\fallingdotseq 0°$) In the case of load ratio, 1/2, the fracture angle, $-\theta_0$ is shown to be between those in the case of the load ratios, 0/1 and 1/1.

Similarly in Fig. 9 (a), (b) and (c), the fracture stresses are plotted against the crack angle, β, by normalizing with respect to fracture stresses when β is 90°, which show almost same values regardless of load ratios. The load ratios in Figs. 9 (a), (b) and (c) are 0/1, 1/2 and 1/1, respectively. The theoretical curves in these figures are also obtained from the criteria in Chapter 2. In the case of uni-axial tension, the fracture stresses increase as the crack angle, β, decreases. When the load ratio is 1/2, the fracture stresses also increase as β decreases, but do not exceed 2.4 times of that for β of 90°. The fracture stresses at the load ratio equal to 1/1 show nearly identical value to that for β of 90°.

From the test results in case of β=90°, no influence can be observed on the fracture stresses with respect to the stresses parallel to the crack direction.

In the following, the three criteria mentioned in Chapter 2 are discussed in comparison with the test results.

(1) $\sigma_{\theta\,max}$ criterion

Erdogan and Sih[1] have studied crack propagation under a general two dimensional stress system. In particular, their work includes the case of a plate under the mixed mode stress system of mode I and II, considering only the first term in Eq. (1). However, Cotterell[7] has discussed the inclusion of other terms with reference to crack direction under simple tension, and has concluded that the second term has a significant effect. Williams and Ewing[2] have also discussed the effect of the second term, and their test results are in good agreement with the theoretical curve when a in Eq. (1) is 0.1.

The test results in this paper are in good agreement with the curves obtained from $\sigma_{\theta\,max}$ criterion when α is 0.1 (r_c=0.1mm). As know from the above discussion, the stresses parallel to the crack direction have a significant effect both on the direction of initial crack propagation and the fracture stress, according to this criterion. However, the physical meaning of r_c of 0.1mm is not clear.

(2) S_{min} criterion

The curves obtained from S_{min} criterion are in good agreement with the test results except the direction of initial crack propagation when the load ratio is 1/2. However, the physical meaning of this criterion is not understandable. Here, the strain energy density around the crak tip is considered. The strain energy density factor, S, can be resolved into two parts, S_V and S_D. S_V is associated with the change in volume, and S_D, the distortion or change in shape of volume element. The variation of S, S_V, S_D and the stress components around the crack tip when crack angle, β, is 30° and the load ratio is 0/1 are shown in Fig. 10. It is found that the variation of total S.E.D.F., S, is dependent mainly upon that of distortion, S_D, and the angle, θ, which minimize the value of S is located near that for minimum S_D.

Now, the deformation which is significant for brittle fracture or cleavage fracture is that of volume change but distortion. When this distortion or change in shape of volume element is confined to the shear deformation, it has an opposite effect on brittle fracture. So, it may be said that the direction of inital crack propagation according to Sih's criterion is close to that of minimum S.E.D.F. for distortion where the brittle fracture occures most easily. Furthermore, this direction is also close to that of maximum tangential stress, $\sigma_{\theta\,max}$. ($\tau_{r\theta}=0$)

(3) $G_{\theta\,max}$ criterion

Judging from curves in Figs. 8 and 9, $G_{\theta\,max}$ criterion predicts fairly accurately the direction of initial crack

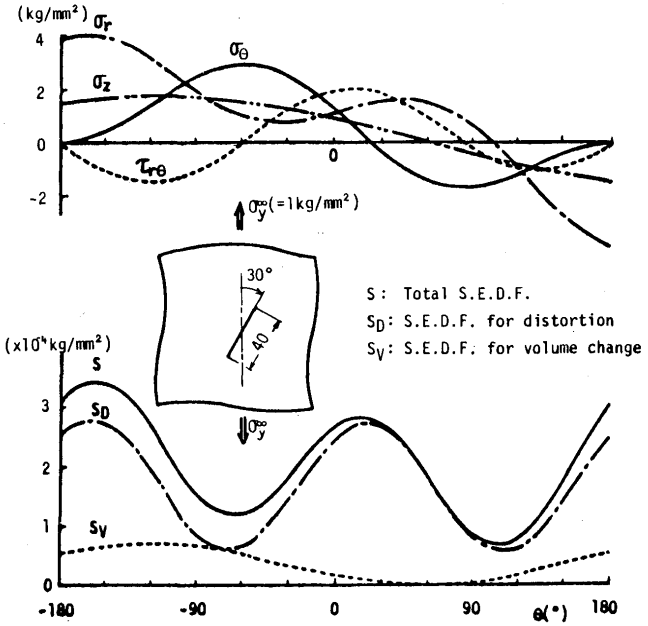

Fig.10 Variation of stresses and strain evergy density factors with crack angle ß (plane strain)

propagation and the fracture stresses obtained from the tests in this study. It is known that $G_{\theta\,max}$ criterion is the most suitable in studying brittle fracture characteristics under the mixed mode stress system. In this study, G_θ can be calculated numerically by using the finite element method. On the othr hand, Nuismer has attempted to express G_θ analytically for a branched crack under a mixed mode stress system of modes I and II as shown in Fig. 3. In the limiting case where Δa tends to zero, the normal and shear stresses, $\sigma_{\bar{y}}$ and $\tau_{\bar{x}\bar{y}}$, at the tip of the branched crack is eualized to those at the tip of the original crack, $\sigma_{\bar{\theta}}$ and $\tau_{r\bar{\theta}}$, along the ray, $\theta=\bar{\theta}$ According to his paper, the stress intensity factor for branched crack at its initiation can be expressed as follows:

$$K_{I\bar{\theta}} = \frac{1}{2}\cos\frac{\theta}{2}\left[K_I(1+\cos\bar{\theta}) - 3K_{II}\sin\bar{\theta})\right]$$
$$K_{II\bar{\theta}} = \frac{1}{2}\cos\frac{\theta}{2}\left[K_I\sin\bar{\theta} + K_{II}(3\cos\bar{\theta} - 1)\right] \qquad (13)$$

where K_I and K_{II} are the stress intensity factors of mode I and II for the original crack, respectively. Having the above stress intensity factors, it is concluded that the decreasing rate of total potential energy, G_θ, due to propagation of the original crack in the direction, $\theta=\bar{\theta}$, is given as

$$G_\theta = \frac{K^2_{I\bar{\theta}} + K^2_{II\bar{\theta}}}{E} \qquad (14)$$

However, the following discussion can be made on his approach. As Kitagawa and Yuki[8] have pointed out in their recent work, the stress intensity factors, $K_{I\bar{\theta}}$ and $K_{II\bar{\theta}}$, have no convergence in the limiting case where Δa is

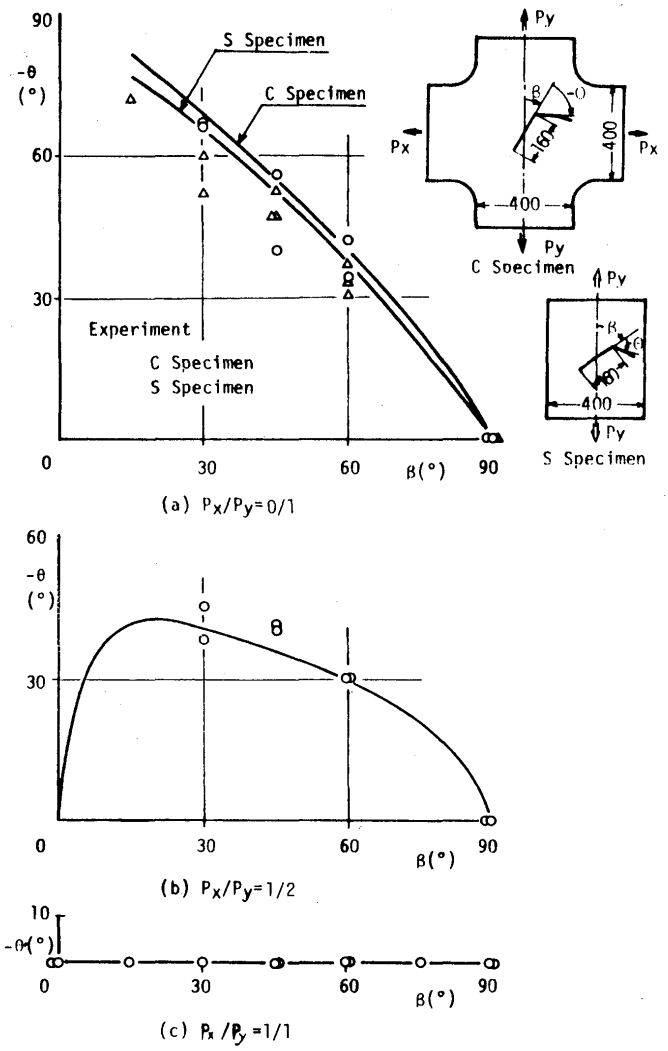

Fig.11 Direction of crack propagation (SM41)

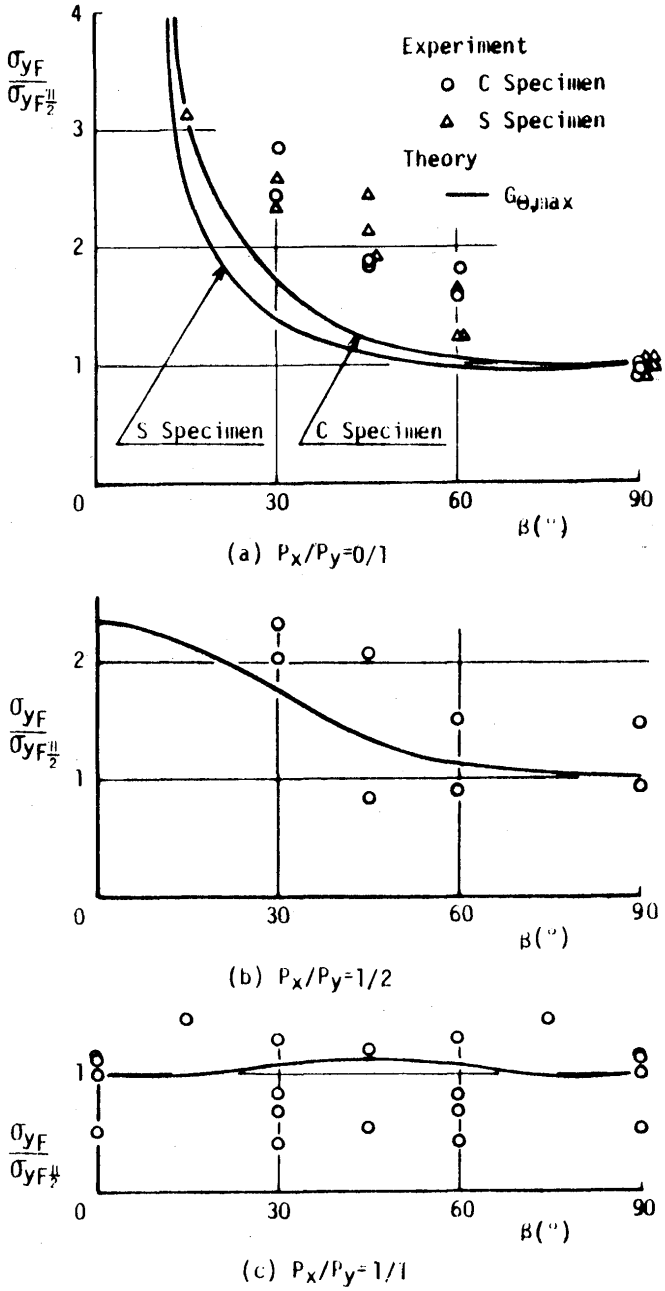

Fig.12 Fracture Stresses non-dimensionalyzed by fracture stress of specimen of ß=90° (SM41)

zero. Furthrmore, the crack opening displacements of branched crack can not be expressed uniquely by the stress intensity factor which prescribes the stress field at the tip of original crack except the case $\bar{\theta}=0$. Therefore, the decreasing rate of total potential energy, G_θ, in the direction of $\theta=\bar{\theta}$ can not be expressed generally in the form of Eq. (14).

4.3 Characteristics of brittle fracture on SM41 specimens under mixed mode stress system

The test results of SM41 specimens are summarized in Figs. 11 and 12 in a similar way to the PMMA specimens. The direction of initial crack propagation is shown in Figs. 11 (a), (b) and (c). The fracture stresses normarized with the fracture stresses obtained from the deep notch test at the same temperature which correspond to the fracture stresses in an infinite plate with a crack, $\beta=90°$ are shown in Figs. 12 (a), (b) and (c). The load ratio in Figs. (a), (b) and (c) of 11 and 12 are 0/1, 1/2 and 1/1, respectively. The theoretical curves in these figures are obtained from G_θ analysis by applying the finite element method, and these curves are in good accordance with the test results as to the direction of initial crack propagation. However, there are some differences between them as far as the fracture stresses are concerned. In the case of load ratio of 1/1, the test results are scattered around the theoretical curve. On the other hand, the experimental data are higher than the theoretical curves when the load ratios are 0/1 and 1/2, and the differences between them are most predominant when the crack angle, β, is 45°. To study these differences, the critical decreasing rate of total potential energy, G_{cr}, are plotted in Fig. 13 against the mode II stress intensity factor K_{II}, by applying the results of G_θ analysis obtained by the finite element method. The same results of PMMA specimens are also shown in this figure.

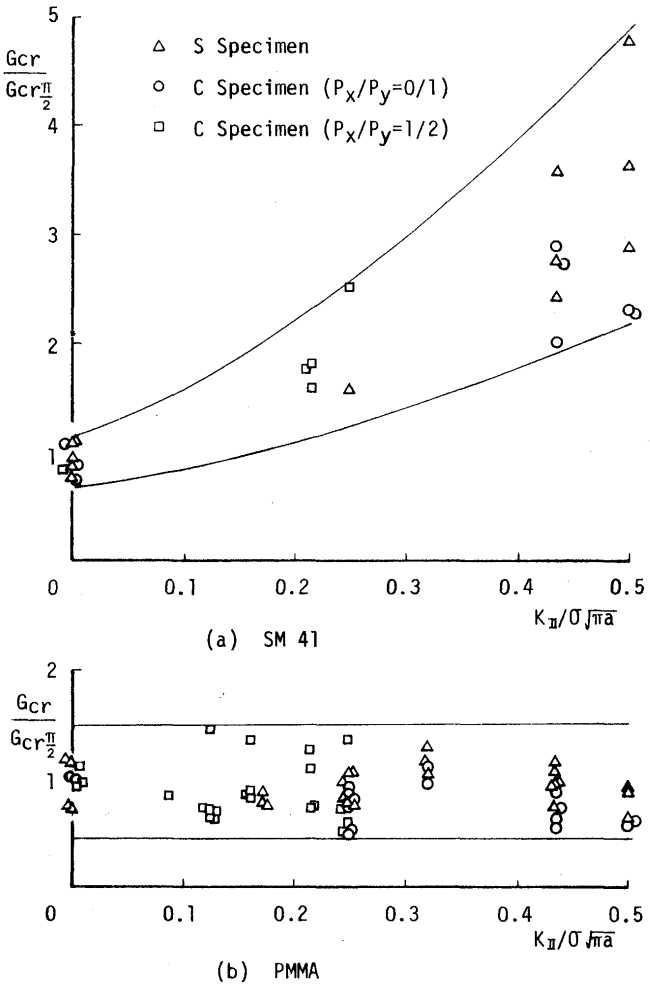

Fig.13 Variation of critical decreasing rate of total potential energy with K_{II}.

In the case of PMMA, which is elastic and perfectly brittle, the slip does not occur, and the energy stored in the core region surrounding the crack tip due to the mode II deformation completely contributes to the released energy at fracture. Therefore, the value of G_{cr} does not show dependency on K_{II} value. On the other hand, in the case of SM41, the stored energy is partly dissipated in forming slip lines. In the ordinary elastic-plastic material such as SM41, the slip lines form at an angle of 45° to the directions of the principal stresses. Consequently, the in-plane shear deformation under mode II stress system changes to this slip most effectively when the direction of slip lines coincide with the original crack direction, $\beta=45°$. This phenomenon is considered one of the main reasons why the critical value of decreasing rate of total potential energy, G_{cr}, increases as the value of K_{II} increases as shown in Fig. 13.

5. Conclusions

Under bi-axial tensile loads, the brittle fracture initiation characteristics of PMMA which is elastic and perfectly brittle material, and mild steel were investigated both theoretically and experimentally. For the fracture tests, a set of newly designed testing machines were employed, which is installed at Welding Research Institute of Osaka University. The following conclusions can be drawn from this study:

(1) The criterion of maximum decrasing rate of total potential energy is the most suitable in predicting the brittle fracture stress and the direction of initial crack propagation under a mixed mode stress system of modes I and II, which is a combination of the opening and in-plane shear modes.

(2) In the case of the load ratio of 1/2, the fracture stress

increases up to 2.4 times that for $\beta=90°$, as the inclination angle of notch to the direction of the main load, β, decreases.

(3) In the case of the load ratio of 1/1, which is equivalent to uniform tension in all directions, the fracture stress does not vary with β, and the direction of initial crack propagation coincides with the line of notch.

(4) In the case of the load ratio of 0/1, that is the uniaxial load, the fracture stress increases as β decreases. However, the direction of initial crack propagation is almost normal to the loading direction irrespective of β.

(5) The uniform stress applied parallel to the line of notch has little effects on the direction of initial crack propagation and the fracture stress.

(6) In the case of an elastic-plastic material such as SM41, the energy stored in the core region surrounding the crack tip is partly dissipated in forming slip lines, and the critical value, G_{cr}, increases as K_{II} value derived from the in-plane shear deformation increases. On the other hand, in the case of elastic and perfectly brittle material such as PMMA, this stored energy completely changes to the released energy at fracture, and the critical value, G_{cr}, does not show the dependency on K_{II} value.

Acknowledgements

The authers wish to express their thanks to Professor T. Kanazawa and the members of Welding Research Committee, the Society of Naval Architects of Japan, for their helpful discussions. The authors highly appreciate the support offered by Professor Emeritus H. Kihara, Professor K. Satoh and Associate Professor M. Toyoda for the installation of the bi-axial tensile testing machine of 300 tons. Further, they thanks Messrs. S. Shibazaki and M. Izaki for their assistance in performance of the experiment.

References

1) F. Erdogan and G. C. Sih: On the Crack Extension in Plates under Plane Loading and Transverse Shear, Trans. ASME, Jour. Basic Eng., 85 D (1963), 519–527.
2) J. G. Williams and P. D. Ewing: Fracture under Complex Stress - the Angled Crack Problem, Int. Jour. Fract. Mech., 8 (1972),441–446.
3) G. C. Sih: Some Basic Problems in Fracture Mechanics and New Concept, Eng. Fract. Mech., 5 (1973),365–377.
4) R. J. Nuismer: An Energy Release Rate Criterion for Mixed Mode Fractures, Int. Jour. Fract. Mech., 11(1975), 245–250.
5) G. P. Anderson. V. L. Ruggles and G. Stibor: Use of Finite Element Computer Programs in Fracture Mechanics, Int. Jour. Fract. Mech., Vol 7, No.1, (1971).
6) I. R. Dixon and L. P. Pook: Stress Intensity Factors Calculated Generally by the Finite Element Technique, Nature, Vol.224, Oct. 11, (1969).
7) B. Cotterell: Notes on the Paths and Stability of Cracks, Int, Jour. Fract. Mech., 2 (1966), 526.
8) H. Kitagawa and R. Yuki: Stress Intensity Factors for Branched Cracks in an Infinite Body in the Two-dimensional Stress State, Bulletin of JSME, Vol.41, No.346 (1975).